JOURNAL OF COMPUTATIONAL PHYSICS **145,** 445–461 (1998)
ARTICLE NO. CP986033

A Rotated Monotone Difference Scheme for the Two-Dimensional Anisotropic Drift-Diffusion Equation

D. Thangaraj and A. Nathan

Department of Electrical and Computer Engineering, University of Waterloo, Waterloo, Ontario, N2L 3G1, Canada
E-mail: tdravia@venus.uwaterloo.ca and anathan@venus.uwaterloo.ca

Received April 7, 1998

A rotated upwind discretization scheme is presented for the discretization of the steady-state two-dimensional anisotropic drift-diffusion equation, taking into account the local characteristic nature of the solution. The notable features of the algorithm lie in the projection of the governing partial differential equation onto two orthogonal axes, to yield a vanishing mixed derivative term, and in the utilization of the upwind flow of information. As a result the limiting behaviour of the elliptic equation is preserved in the discretization. The scheme produces an M-matrix which guarantees an oscillation free solution and which enables the discrete system to be solved using standard iterative solvers. The method is illustrated by numerical examples for which the analytical solutions are known.

1. INTRODUCTION

This paper describes a new rotated monotone finite-difference scheme for solving the two-dimensional, steady-state, anisotropic elliptic partial differential equation (PDE)

$$-A_1(x,y)\frac{\partial^2\phi}{\partial x^2} - A_2(x,y)\frac{\partial^2\phi}{\partial x\,\partial y} - A_3(x,y)\frac{\partial^2\phi}{\partial y^2} + A_4(x,y)\frac{\partial\phi}{\partial x} + A_5(x,y)\frac{\partial\phi}{\partial y} + A_6(x,y)\,\phi = 0 \qquad \text{in } \Omega \tag{1}$$

subject to a mixture of Dirichlet and Neumann boundary conditions. Here, the A_i $(i = 1, \ldots, 6)$ are known functions of the independent variables defined on a domain Ω on whose boundary $\partial\Omega$, the boundary conditions are prescribed. The coefficients of the second derivative terms of the PDE, generally called diffusion coefficients, are given so that the PDE represents an elliptic equation, i.e., $A_2^2 - 4A_1A_3 < 0$ at any point (x, y). For convenience, it is assumed that the coefficients $A_1(x, y)$ and $A_3(x, y)$ are of same sign and are positive.

0021-9991/98 $25.00

The linear source term $A_6(x, y)$ is also assumed positive so that the maximum principle can be attained. The coefficients of the first derivatives, called drift velocity components, convect the unknown dependent variable ϕ.

The above PDE arises in many branches of engineering physics. For example, when a semiconductor device is subject to a magnetic field, the current density relations, and hence, the current continuity equations for electrons and holes, become anisotropic by virtue of the Lorentz force [1,2]. Similarly, in the presence of mechanical stress, carrier transport in the semiconductor device becomes anisotropic by virtue of piezoresistance [3]. The anisotropic diffusion equation also governs flow in porous media, pertinent to reservoir simulation problems, as well as the transport of atmospheric gases [4,5]. The PDE (1) is called the Hamilton–Jacobi–Bellman equation which governs the dynamics of any stochastic optimal control problem when the underlying processes are driven by Brownian motion [6].

In discretization of the PDE, we seek the resultant discrete system to be an M-matrix so as to enable use of standard iterative algorithms based on Gauss–Seidel methods. In addition, the M-matrix guarantees the discrete maximum principle. In the absence of a source term, the maximum principle states that the maximum of the unknown dependent variable occurs on the boundary and that the dependent variable does not take negative values. If the discretization scheme does not preserve this property, then the solutions may take negative values and oscillate, which may not be meaningful from both physical and mathematical points of view [7,8]. To attain this maximum principle, the discrete set of equations should satisfy the following properties [7,8]:

(1) Diagonal entries of all rows should be positive.
(2) Off-diagonal entries of all rows should be non-positive.
(3) Sum of entries of any row should be non-negative, but this sum should be positive for at least one row.

If a discrete system satisfies the above conditions, the matrix is said to be an M-matrix, the inverse of which contains only positive entries. Many numerical methods have been proposed for the discretization of the PDE [9,10]. The presence of the mixed derivative term limits the attaining of an M-matrix, although there are many schemes that satisfy various stability criteria needed for an M-matrix. However, the schemes do not take into account the special features of the PDE except its elliptic nature. In addition, the presence of the first derivative terms imposes conditions on the mesh size to obtain an M-matrix using central difference formulas. The usual upwind schemes to deal with the first derivative terms do not accurately model the local characteristics of the PDE.

The objective of this work is to develop a rotated monotone discretization scheme for the anisotropic elliptic PDE taking into account the local characteristic nature of the solution to yield a resultant discrete system that is an M-matrix. There are two rotations in this scheme. One rotation pertains to the projection of the diffusion part of the PDE along the orthogonal axes so that the mixed derivative term vanishes in the new coordinate system. The other rotation addresses the discretization of the convective derivative. Section 2 describes the numerical issues associated with the discretization of the mixed derivative term in conjunction with a diffusion equation with constant but anisotropic coefficients. The numerical issues can be overcome using a physically stable rotated monotone difference scheme. This is presented in Section 3. Section 4 deals with the discretization of the generalized two-dimensional anisotropic convective diffusion equation by a rotated upwind

scheme that produces an M-matrix. As illustrations of the method, numerical examples are given in Section 5.

2. NUMERICAL ISSUES IN THE DISCRETIZATION OF THE MIXED DERIVATIVE TERM

In this section we analyze the numerical issues associated with the discretization of a simple, two-dimensional, steady state, anisotropic diffusion equation. The anisotropic diffusion problem is defined by

$$J_x = D_{11}\frac{\partial \phi}{\partial x} + D_{12}\frac{\partial \phi}{\partial y} \tag{2}$$

$$J_y = D_{21}\frac{\partial \phi}{\partial x} + D_{22}\frac{\partial \phi}{\partial y} \tag{3}$$

$$-\frac{\partial J_x}{\partial x} - \frac{\partial J_y}{\partial y} = 0, \tag{4}$$

where the D_{ij} $(i = 1, 2, j = 1, 2)$ are diffusion coefficients which make the conservation equation (4) elliptic, and J_x and J_y are the typical diffusion flux vector components influencing the potential ϕ. The above problem is solved in a rectangular domain $\Omega = \{(x, y)/a \le x \le b, c \le y \le d\}$ subject to a mixture of Dirichlet and Neumann boundary conditions. For simplicity we assume

$$\phi = \phi_B \text{ at } x = a \quad \text{and} \quad x = b \quad \text{for } c \le y \le d \tag{5}$$

$$J_y = Q_B \text{ at } y = c \quad \text{and} \quad y = d \quad \text{for } a \le x \le b, \tag{6}$$

where ϕ_B is a known function on the Dirichlet boundary, and Q_B is a prescribed flux function on the Neumann boundary. Substituting for the flux components in (4), the governing equation can be cast in the form

$$-A_1\frac{\partial^2 \phi}{\partial x^2} - A_2\frac{\partial^2 \phi}{\partial x\,\partial y} - A_3\frac{\partial^2 \phi}{\partial y^2} = 0, \qquad \text{in } \Omega, \tag{7}$$

where the coefficient A_i are given by $A_1 = D_{11}$, $A_2 = D_{11} + D_{12}$, $A_3 = D_{22}$.

The PDE (7) is discretized over a rectangular grid. Following the notation used for the various nodes surrounding the interior node (i, j) as shown in Fig. 1, the second derivatives along the coordinate axes are discretized by

$$\frac{\partial^2 \phi}{\partial x^2}(x_i, y_j) = \frac{\phi_{i+1,j} - 2\phi_{i,j} + \phi_{i-1,j}}{h^2} \tag{8}$$

and

$$\frac{\partial^2 \phi}{\partial y^2}(x_i, y_j) = \frac{\phi_{i,j+1} - 2\phi_{i,j} + \phi_{i,j-1}}{k^2}, \tag{9}$$

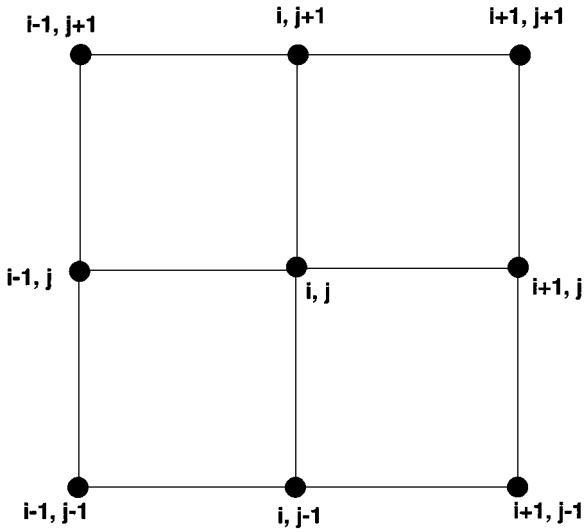

FIG. 1. Grid used in numerical scheme indicating notation used for nodes surrounding the central node (i, j).

where $\phi_{i,j}$ is the dependent variable defined at node (i, j), and $x_{i+1} - x_i = h$ and $y_{j+1} - y_j = k$. The mixed derivative is discretized by the second-order accurate scheme

$$\frac{\partial^2 \phi}{\partial x\, \partial y}(x_i, y_j) = \frac{\phi_{i+1,j+1} + \phi_{i-1,j-1} - \phi_{i+1,j-1} - \phi_{i-1,j+1}}{4hk}. \tag{10}$$

At the Dirichlet boundary nodes, we have

$$\phi_{i,j} = \phi_B,$$

where ϕ_B is known. At nodes on the boundary that lie parallel to the x-axis and form part of the upper boundary ($y = d$), the insulating boundary condition

$$J_y = D_{21}\frac{\partial \phi}{\partial x} + D_{22}\frac{\partial \phi}{\partial y} = 0$$

is discretized as follows. When both D_{22} and D_{21} are of the same sign, the insulating boundary condition is discretized as

$$D_{21}\left(\frac{\phi_{i,j} - \phi_{i-1,j}}{h}\right) + D_{22}\left(\frac{\phi_{i,j} - \phi_{i,j-1}}{k}\right) = 0. \tag{11}$$

When both D_{22} and D_{21} are of different sign, the discretized insulating boundary condition is given by

$$D_{21}\left(\frac{\phi_{i+1,j} - \phi_{i,j}}{h}\right) + D_{22}\left(\frac{\phi_{i,j} - \phi_{i,j-1}}{k}\right) = 0. \tag{12}$$

Similarly, we can discretize the Neumann boundary condition at the other boundary $y = d$. Substituting (8)–(10) into (7) at all interior points (i, j), the discretized equation is given

by

$$-A_1\left\{\frac{\phi_{i+1,j}-2\phi_{i,j}+\phi_{i-1,j}}{h^2}\right\}-A_2\left\{\frac{\phi_{i+1,j+1}+\phi_{i-1,j-1}-\phi_{i+1,j-1}-\phi_{i-1,j+1}}{4hk}\right\}$$
$$-A_3\left\{\frac{\phi_{i,j+1}-2\phi_{i,j}+\phi_{i,j-1}}{k^2}\right\}=0. \tag{13}$$

For any row, associated with the interior node (i, j), the diagonal entry is given by $2A_1/h^2+2A_3/k^2$, which is positive irrespective of h and k. But the off-diagonal entries $-A_2/4hk$ corresponding to the nodes $(i+1, j+1)$ and $(i-1, j-1)$ always differ in sign from the entries $A_2/4hk$ corresponding to the nodes $(i+1,\ j-1)$ and $(i-1, j+1)$. Hence the discrete system will never be an M-matrix irrespective of the grid size h and k. This hurdle is purely due to the way the mixed derivative term is discretized. This is precisely the reason Tapiero and Sulem [6], Asencor and Panizo [11], and Crumpton *et al.* [4] could not attain discrete maximum principles in their discretization. It may be noted here that the above conclusion is independent of the way the Neumann boundary condition (6) is discretized. Other discretization schemes for the mixed derivative include [9]

$$\frac{\partial^2\phi}{\partial x\,\partial y}(x_i,y_j)=\frac{\phi_{i+1,j+1}+\phi_{i-1,j-1}-\phi_{i+1,j}-\phi_{i-1,j}-\phi_{i,j+1}-\phi_{i,j-1}+2\phi_{i,j}}{2hk} \tag{14}$$

$$\frac{\partial^2\phi}{\partial x\,\partial y}(x_i,y_j)=\frac{\phi_{i,j+1}+\phi_{i,j-1}+\phi_{i-1,j}+\phi_{i+1,j}-\phi_{i-1,j+1}-\phi_{i+1,j-1}-2\phi_{i,j}}{2hk} \tag{15}$$

$$\frac{\partial^2\phi}{\partial x\,\partial y}(x_i,y_j)=\frac{\phi_{i+1,j+1}+\phi_{i,j}-\phi_{i,j+1}-\phi_{i+1,j}}{hk} \tag{16}$$

$$\frac{\partial^2\phi}{\partial x\,\partial y}(x_i,y_j)=\frac{\phi_{i,j+1}+\phi_{i-1,j}-\phi_{i,j}-\phi_{i-1,j+1}}{hk} \tag{17}$$

$$\frac{\partial^2\phi}{\partial x\,\partial y}(x_i,y_j)=\frac{\phi_{i,j}+\phi_{i-1,j-1}-\phi_{i,j-1}-\phi_{i-1,j}}{hk} \tag{18}$$

$$\frac{\partial^2\phi}{\partial x\,\partial y}(x_i,y_j)=\frac{\phi_{i+1,j}+\phi_{i,j-1}-\phi_{i,j}-\phi_{i+1,j-1}}{hk}. \tag{19}$$

The above schemes are of different accuracy varying from first order to second order. But all of them, along with schemes (8) and (9), produce the M-matrix under restricted conditions:

(1) If A_1, A_2, and A_3 are all positive, scheme (14) will produce an M-matrix if

$$\frac{A_2}{2hk}\le\min\left\{\frac{A_1}{h^2},\frac{A_3}{k^2}\right\} \tag{20}$$

but not when A_2 is negative.

(2) If A_1, A_3 are positive and A_2 is negative, scheme (15) will produce an M-matrix if

$$-\frac{A_2}{2hk}\le\min\left\{\frac{A_1}{h^2},\frac{A_3}{k^2}\right\} \tag{21}$$

but not when A_2 is positive.

(3) If A_1, A_2, and A_3 are all positive, schemes (16) and (18) will produce an M-matrix if

$$\frac{A_2}{hk} \leq \min\left\{\frac{A_1}{h^2}, \frac{A_3}{k^2}\right\} \tag{22}$$

but not when A_2 is negative.

(4) If A_1, A_3 are positive and A_2 is negative, schemes (17) and (19) will produce an M-matrix if

$$-\frac{A_2}{hk} \leq \min\left\{\frac{A_1}{h^2}, \frac{A_3}{k^2}\right\} \tag{23}$$

but not when A_2 is positive.

The discretization schemes (14)–(19) for the mixed derivative term hold for any arbitrary elliptic PDE. The schemes do not take into account the special features of the governing PDE except its elliptic nature. However, the elliptic nature of the equation, quantified by the term $A_2^2 - 4A_1A_3$, weakens as the anisotropy, represented by the coefficient of the mixed derivative term, dominates in magnitude. As the coefficient of the mixed derivative term increases, $A_2^2 - 4A_1A_3 \to 0$, thus weakening the elliptic nature. In this limit, the governing elliptic equation becomes an ordinary differential equation along some axis defined by the diffusion coefficients. In this limiting case, any interior point is heavily influenced by neighborhood points on the axis, and not by the other surrounding points. This onset of parabolic nature of the elliptic PDE should be taken into account when devising the numerical schemes. This is illustrated in the next section.

3. A ROTATED DIFFERENCE FOR THE ANISOTROPIC DIFFUSION EQUATION

In this section, we present a physically rotated difference scheme that incorporates the limiting characteristics of the anisotropic diffusion equation. The governing diffusion equation (7) is cast in the form

$$\left\{-B\frac{\partial^2\phi}{\partial x^2} - A_2\frac{\partial^2\phi}{\partial x\,\partial y} - \frac{A_2^2}{4B}\frac{\partial^2\phi}{\partial y^2}\right\} + (B - A_1)\frac{\partial^2\phi}{\partial x^2} + \left(\frac{A_2^2}{4B} - A_3\right)\frac{\partial^2\phi}{\partial y^2} = 0, \tag{24}$$

where B is any arbitrary constant selected so that

$$\frac{A_2^2}{4A_3} \leq B \leq A_1. \tag{25}$$

We split the governing equation so that the limiting elliptic behaviour is represented exactly. It can be seen that the part

$$-B\frac{\partial^2\phi}{\partial x^2} - A_2\frac{\partial^2\phi}{\partial x\,\partial y} - \frac{A_2^2}{4B}\frac{\partial^2\phi}{\partial y^2}$$

is always parabolic, when it is considered alone, irrespective of B. This part of the PDE is projected along two orthogonal coordinate systems so that the mixed derivative term

vanishes in the transformed system given by

$$u = x\cos\theta + y\sin\theta$$
$$v = -x\sin\theta + y\cos\theta$$

along with

$$\tan 2\theta = \frac{A_2}{B - A_2^2/4B}. \tag{26}$$

This leads to

$$\tan\theta = \frac{A_2}{2B} \tag{27}$$

and

$$\tan\theta = -\frac{2B}{A_2}. \tag{28}$$

Along the direction defined by (27), the partial differential equation (24) becomes

$$-P_1\frac{\partial^2\phi}{\partial u^2} + (B - A_1)\frac{\partial^2\phi}{\partial x^2} + \left(\frac{A_2^2}{4B} - A_3\right)\frac{\partial^2\phi}{\partial y^2} = 0, \tag{29}$$

where

$$P_1 = \cos^2\theta\left\{B + \frac{A_2^2}{2B} + \frac{A_2^4}{16B^3}\right\}.$$

Along the direction defined by (28), the governing equation may be represented by

$$-P_2\frac{\partial^2\phi}{\partial v^2} + (B - A_1)\frac{\partial^2\phi}{\partial x^2} + \left(\frac{A_2^2}{4B} - A_3\right)\frac{\partial^2\phi}{\partial y^2} = 0, \tag{30}$$

where

$$P_2 = \cos^2\theta\left\{2B + \frac{A_2^2}{4B} + \frac{4B^3}{A_2^2}\right\}.$$

However, since both Eqs. (29) and (30) are similar, our analysis is restricted to (29) with the rotation angle given by (27). The second derivative of ϕ along the u-axis needs to be discretized on a rectangular grid; hence, at least two nodes must lie on that axis. This takes place if

$$|\tan\theta| = \frac{|A_2|}{2B} = \frac{k}{h}. \tag{31}$$

Using this, the inequality (25) leads to

$$\frac{|A_2|}{2A_1} \le \frac{k}{h} \le \frac{2A_3}{|A_2|}. \tag{32}$$

This is the stability criterion required to produce a discrete M-matrix. As $A_2 \to 0$, anisotropy decreases and the choice of ratio of step sizes is no longer constrained. Once the ratio between the step sizes has been selected, the arbitrary constant B can also be fixed using

$$B = \frac{|A_2|h}{2k}. \tag{33}$$

When the rotation angle is positive, the second derivative of ϕ along the u-axis can be discretized as

$$\frac{\partial^2 \phi}{\partial u^2}(i, j) = \frac{\phi_{i+1,j+1} - 2\phi_{i,j} + \phi_{i-1,j-1}}{s^2}, \tag{34}$$

where s is the distance between nodes (i, j) and $(i+1, j+1)$. When the rotation angle is negative, the derivative is given by

$$\frac{\partial^2 \phi}{\partial u^2}(i, j) = \frac{\phi_{i+1,j-1} - 2\phi_{i,j} + \phi_{i-1,j+1}}{s^2}. \tag{35}$$

The differential operators along the orthogonal axes can be discretized as usual; see (8) and (9). Substituting (8), (9), and (34) into (29), the discretized equation for positive rotation angle becomes

$$\begin{aligned}
&\left\{\frac{2P_1}{s^2} - \frac{2(B - A_1)}{h^2} - \frac{2\left(A_2^2/4B - A_3\right)}{k^2}\right\}\phi_{i,j} - \left\{\frac{(B - A_1)}{h^2}\right\}\phi_{i+1,j} - \left\{\frac{P_1}{s^2}\right\}\phi_{i+1,j+1} \\
&\quad - \left\{\frac{(B - A_1)}{h^2}\right\}\phi_{i-1,j} - \left\{\frac{P_1}{s^2}\right\}\phi_{i-1,j-1} - \left\{\frac{\left(A_2^2/4B - A_3\right)}{k^2}\right\}\phi_{i,j+1} \\
&\quad - \left\{\frac{\left(A_2^2/4B - A_3\right)}{k^2}\right\}\phi_{i,j-1} = 0.
\end{aligned} \tag{36}$$

It can be noted that the coefficients of $\phi_{i+1,j+1}$, $\phi_{i+1,j}$, $\phi_{i-1,j}$, $\phi_{i-1,j-1}$, $\phi_{i,j+1}$, and $\phi_{i,j-1}$ are all non-positive. Also the sum of the entries in each row, corresponding to every interior node (i, j), is zero. The discretization of Dirichlet and Neumann boundary conditions (11) and (12) on the boundary nodes guarantee the remaining requirements for the discrete system to be an M-matrix.

If the diffusion coefficients A_1, A_2, and A_3 are functions of the coordinates x and y, the stability criterion (32) becomes

$$\mathrm{Max}_{i,j}\left\{\frac{|A_2(i, j)|}{2A_1(i, j)}\right\} \le \frac{k}{h} \le \mathrm{Min}_{i,j}\left\{\frac{2A_3(i, j)}{|A_2(i, j)|}\right\} \tag{37}$$

and the associated B at any node (i, j) is given by

$$B(i, j) = \frac{|A_2(i, j)|h}{2k}. \tag{38}$$

This means that the function $B(x, y)$ for a fixed grid will depend on $A_2(x, y)$ at any interior point.

4. A ROTATED UPWIND SCHEME FOR THE 2D ANISOTROPIC DRIFT-DIFFUSION EQUATION

Following the results obtained in the previous section, we describe a monotone rotated upwind discretization scheme for the anisotropic drift-diffusion equation (1), subject to the Dirichlet and Neumann boundary conditions (5) and (6).

We select the ratio of step sizes so that it satisfies the stability condition (37). At any interior node (i, j), with the coordinate (x_i, y_j), the second derivative terms in Eq. (1) can be written as

$$\begin{aligned} &-A_1(i,j)\frac{\partial^2\phi}{\partial x^2} - A_2(i,j)\frac{\partial^2\phi}{\partial x\,\partial y} - A_3(i,j)\frac{\partial^2\phi}{\partial y^2} \\ &\quad = -P_1(i,j)\frac{\partial^2\phi}{\partial u^2} + \left(B(i,j) - A_1(i,j)\right)\frac{\partial^2\phi}{\partial x^2} + \left(\frac{A_2^2(i,j)}{4B(i,j)} - A_3(i,j)\right)\frac{\partial^2\phi}{\partial y^2}, \end{aligned} \tag{39}$$

where $B(i, j)$ is given by (38) and

$$P_1(i,j) = \cos^2\theta\left\{B(i,j) + \frac{A_2^2(i,j)}{2B(i,j)} + \frac{A_2^4(i,j)}{16B^3(i,j)}\right\}.$$

Depending on the sign of the rotation angle, defined by

$$\tan\theta = \frac{A_2(i,j)}{2B(i,j)}, \tag{40}$$

the second derivative operator along the u-axis and other two orthogonal axes are discretized as explained in the previous section. To discretize the convective derivative terms, the convective part of Eq. (1) is cast in the form

$$A_4\frac{\partial\phi}{\partial x}(x_i, y_j) + A_5\frac{\partial\phi}{\partial y}(x_i, y_j) = \sqrt{A_4^2 + A_5^2}\,\frac{\partial\phi}{\partial s}(i,j), \tag{41}$$

where $\frac{\partial\phi}{\partial s}$ is the derivative of ϕ in the direction of the characteristic given by

$$\frac{du}{A_4} = \frac{dv}{A_5}.$$

The characteristic derivative $\frac{\partial\phi}{\partial s}$ at $O(i, j)$ is then discretized by

$$\frac{\partial\phi}{\partial s} = \frac{\phi(O) - \phi(P)}{d_{OP}}, \tag{42}$$

where d_{OP} is the distance between O and P. The root of the characteristic P need not be a nodal point when the characteristic curve does not coincide with one of the diagonals of the polygon. The characteristic line, OP (where P is an arbitrary point denoting the intersection of the local characteristic with the boundary of the cell), is assumed to be linear within the cell connecting the eight surrounding nodes. The location of P depends on the sign of $A_4(i, j)$ and $A_5(i, j)$:

(1) When both $A_4(i, j)$ and $A_5(i, j)$ are negative, P either lies on the line joining the nodes $(i + 1, j)$ and $(i + 1, j + 1)$ or that of the nodes $(i + 1, j + 1)$ and $(i, j + 1)$.

(2) When $A_4(i, j)$ is positive and $A_5(i, j)$ is negative, P either lies on the line joining the nodes $(i, j+1)$ and $(i-1, j+1)$ or that of the nodes $(i-1, j+1)$ and $(i-1, j)$.

(3) When both $A_4(i, j)$ and $A_5(i, j)$ are positive, P either lies on the line joining the nodes $(i-1, j)$ and $(i-1, j-1)$ or that of the nodes $(i-1, j-1)$ and $(i, j-1)$.

(4) When $A_4(i, j)$ is negative and $A_5(i, j)$ is positive, P either lies on the line joining the nodes $(i, j-1)$ and $(i+1, j-1)$ or that of the nodes $(i+1, j-1)$ and $(i+1, j)$.

When the characteristic does not coincide with the co-ordinate axes, P has to be interpolated between the neighboring nodes and this can be done in many ways. In this work, a linear interpolation is employed. We will illustrate this with an example. Let the characteristic meet the line connecting the nodes $(i+1, j)$ and $(i+1, j+1)$ at P for the case when $A_4(i, j)$ and $A_5(i, j)$ are negative. Expanding by Taylor's series and neglecting the higher order terms, we get

$$\phi(P) = \frac{y_P - y_j}{k}\phi_{i+1,j+1} + \frac{y_{j+1} - y_P}{k}\phi_{i+1,j}.$$

When the interior node is near the boundary, there will not be eight neighboring nodes, if the domain is not rectangular, and $\phi(P)$ has to be interpolated accordingly. When the convective velocity is in the direction of one of the coordinate axes, the scheme reduces to the usual first order upwinding. In many respects the discretization employed here is along the lines proposed by Rice and Schnipke [12] for the discretization of isotropic elliptic partial differential equation and used by Roe and Sidilkover [13] for the discretization of hyperbolic equations. Combining the discretization of the diffusive and convective derivative terms, we get

$$\begin{aligned} C_{i,j}\phi_{i,j} = {} & C_{i-1,j-1}\phi_{i-1,j-1} + C_{i,j-1}\phi_{i,j-1} + C_{i+1,j-1}\phi_{i+1,j-1} + C_{i+1,j}\phi_{i+1,j} \\ & + C_{i+1,j+1}\phi_{i+1,j+1} + C_{i,j+1}\phi_{i,j+1} + C_{i-1,j+1}\phi_{i-1,j+1} + C_{i-1,j}\phi_{i-1,j}, \end{aligned} \quad (43)$$

where

$$\begin{aligned} C_{i,j} &= C_{i-1,j-1} + C_{i,j-1} + C_{i+1,j-1} + C_{i+1,j} + C_{i+1,j+1} + C_{i,j+1} \\ &\quad + C_{i-1,j+1} + C_{i-1,j} + A_6(i, j) \\ C_{i-1,j-1} &= \frac{P_1(i, j)}{s^2} \\ C_{i,j-1} &= \frac{\left(A_2^2(i, j)/4B(i, j) - A_3(i, j)\right)}{k^2} \\ C_{i+1,j-1} &= 0 \\ C_{i+1,j} &= \frac{(B(i, j) - A_1(i, j))}{h^2} + \sqrt{A_4^2(i, j) + A_5^2(i, j)}\,\frac{y_{j+1} - y_P}{d_{OP}k} \\ C_{i+1,j+1} &= \frac{P_1(i, j)}{s^2} + \sqrt{A_4^2(i, j) + A_5^2(i, j)}\,\frac{y_P - y_j}{d_{OP}k} \\ C_{i,j+1} &= \frac{\left(A_2^2(i, j)/4B(i, j) - A_3(i, j)\right)}{k^2} \\ C_{i-1,j+1} &= 0 \\ C_{i-1,j} &= \frac{(B(i, j) - A_1(i, j))}{h^2}. \end{aligned}$$

All of the off-diagonal entries are non-positive. Also the sum of the entries of each row, corresponding to every interior node (i, j), is zero. The Dirichlet and Neumann boundary conditions on the boundary nodes guarantee the remaining requirements for the discrete system to be an M-matrix.

5. NUMERICAL ILLUSTRATIONS

In order to test and validate the accuracy of the numerical solution, the scheme has been applied to extreme or limiting conditions, such as pure diffusion and pure convection problems, for which analytical solutions are known. In the pure convection case, with a known convective velocity along the diagonal of the unit cell, the scheme was able to predict the exact solution even when the analytical solution was discontinuous across the diagonal. Similarly the scheme was tested for purely diffusion controlled problems ($A_4 = A_5 = A_6 = 0$) with constant coefficients. Here, the analytic solution is given by

$$\phi = a_0 + a_1 x + a_2 y + a_3 x^2 + a_4 xy + a_5 y^2$$

with

$$a_5 = -\frac{A_1 2a_3 + A_2 a_4}{2A_3},$$

where $a_i (i = 0, \ldots, 4)$ are arbitrary constants. The Dirichlet condition is selected consistently with the analytical solution. The numerical solution coincides with the exact solution for arbitrary coefficients of the differential equation.

In the third test case, we consider a problem whose coefficients of the PDE, $A_i(x, y)$ $(i = 1, \ldots, 5)$ are constants and $A_6 = 0$. One possible solution is obtained as follows. Using an orthogonal transformation given by

$$\begin{aligned} u &= x \cos\theta + y \sin\theta \\ v &= -x \sin\theta + y \cos\theta \end{aligned}$$

with

$$\tan 2\theta = \frac{A_2}{A_1 - A_3},$$

the PDE (1) is cast in the form

$$P\frac{\partial^2 \phi}{\partial u^2} + Q\frac{\partial^2 \phi}{\partial v^2} + R\frac{\partial \phi}{\partial u} + S\frac{\partial \phi}{\partial v} = 0, \tag{44}$$

where

$$\begin{aligned} -P &= A_1 \cos^2\theta + A_2 \sin\theta \cos\theta + A_3 \sin^2\theta \\ -Q &= A_1 \sin^2\theta - A_2 \sin\theta \cos\theta + A_3 \cos^2\theta \\ R &= A_4 \cos\theta + A_5 \sin\theta \\ S &= -A_4 \sin\theta + A_5 \cos\theta. \end{aligned}$$

A general solution can be obtained by the method of separation of variables. Assuming the solution to be of product form

$$\phi(u, v) = G(u)H(v)$$

we get, when $\phi \neq 0$

$$P\frac{d^2G}{du^2} + R\frac{dG}{du} - \alpha G = 0$$

$$Q\frac{d^2H}{dv^2} + S\frac{dH}{dv} + \alpha H = 0,$$

where α is any arbitrary parameter independent of u and v. Since the original PDE is elliptic in nature, the coefficients P and Q will be of the same sign. For convenience, we assume that P and Q are negative. Depending on α, we may get different families of solutions. We will restrict our attention to the case $\alpha_1 \leq \alpha \leq \alpha_2$, where

$$\alpha_1 = \frac{S^2}{4Q}, \qquad \alpha_2 = -\frac{R^2}{4P}.$$

This interval will cover most of the region of interest for α when the diffusion terms tend to shrink in magnitude compared to the drift terms. The solution is given by

$$\phi(u, v) = \beta_1(\alpha)\, e^{m_1 u + n_1 v} + \beta_2(\alpha)\, e^{m_1 u + n_2 v} + \beta_3(\alpha)\, e^{m_2 u + n_1 v} + \beta_4(\alpha)\, e^{m_2 u + n_2 v},$$

where

$$m_1 = \frac{-R + \sqrt{R^2 + 4P\alpha}}{2P} \qquad m_2 = \frac{-R - \sqrt{R^2 + 4P\alpha}}{2P}$$

$$n_1 = \frac{-S + \sqrt{S^2 - 4Q\alpha}}{2Q} \qquad n_2 = \frac{-S - \sqrt{S^2 - 4Q\alpha}}{2Q}.$$

Here, $\beta_1(\alpha)$, $\beta_2(\alpha)$, $\beta_3(\alpha)$, $\beta_4(\alpha)$ are arbitrary functions of the parameter α and the general solution is given by

$$\phi(u, v) = \int_{\alpha_1}^{\alpha_2} \left\{ \beta_1(\alpha)\, e^{m_1 u + n_1 v} + \beta_2(\alpha)\, e^{m_1 u + n_2 v} + \beta_3(\alpha)\, e^{m_2 u + n_1 v} + \beta_4(\alpha)\, e^{m_2 u + n_2 v} \right\} d\alpha. \tag{45}$$

This analytical solution is applied as Dirichlet boundary conditions with

$$\beta_1(\alpha) = \beta_2(\alpha) = \beta_3(\alpha) = \beta_4(\alpha) = \delta(\alpha - \alpha_0),$$

where $\delta(\alpha - \alpha_0)$ is the Kronecker delta function and $\alpha_0 = \frac{\alpha_1 + \alpha_2}{2}$.

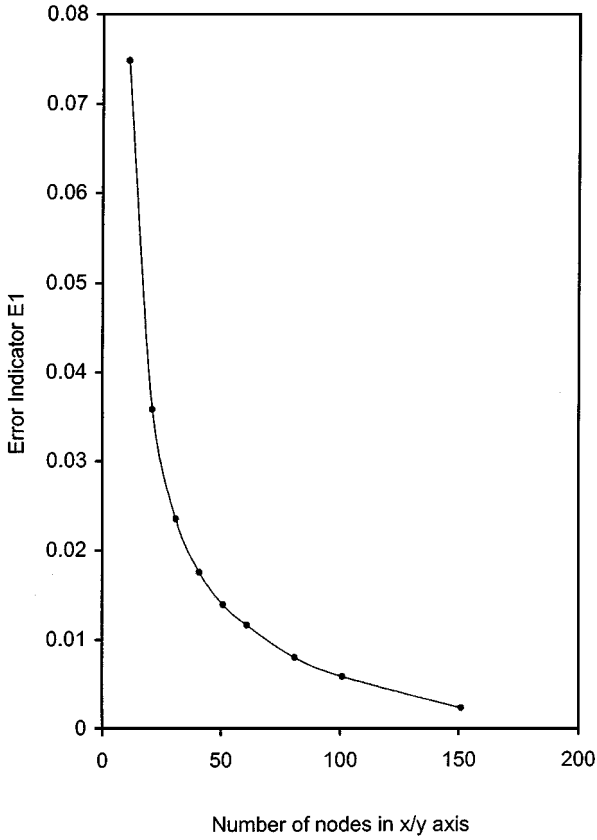

FIG. 2. The error indicator E1, described by Eq. (46), as a function of node density in x- and y-directions, for the test problem $A_1 = 1.0$, $A_2 = 1.8$, $A_3 = 1.0$, $A_4 = 2.0$, $A_5 = 2.0$.

To determine the integrity of the discretization scheme, we employ the standard error indicators

$$E1 = \frac{\sum |\phi(i) - \Psi(i)|}{N} \tag{46}$$

$$E2 = \frac{|\phi(i) - \Psi(i)|}{\Psi(i)}, \tag{47}$$

where the relative error is defined for the non-vanishing exact solution. Here, the summation is over the total number of nodes N, and $\phi(i)$ and $\Psi(i)$ are the numerical and the exact solutions at a discrete node i, respectively. All computations are carried out on a unit square and the Gauss–Seidel method is considered to have converged to the solution when

$$\frac{\sum |\phi(i)^{k+1} - \phi(i)^k|}{N} < 2.5 \times 10^{-7}. \tag{48}$$

Here, the index k denotes the iteration number.

To validate our numerical discretization scheme, we employ relations (46) and (47) on two test cases, for which the analytical solutions are given by Eq. (45). In both cases, we

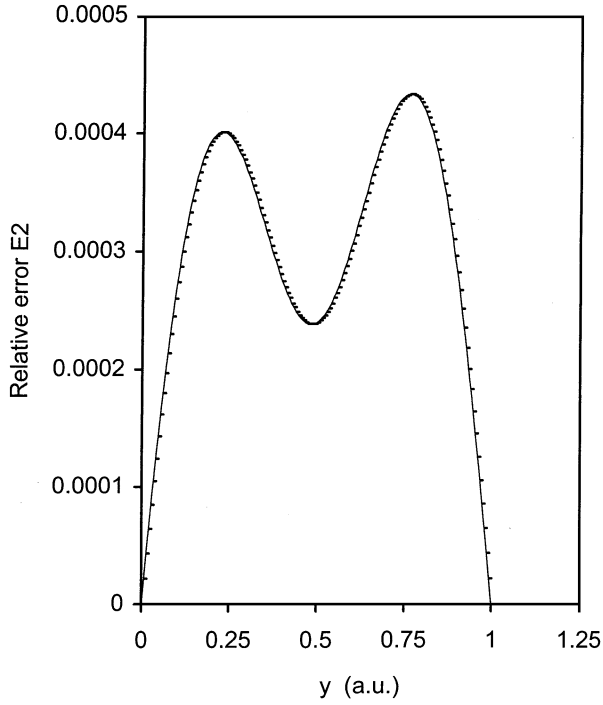

FIG. 3. The relative error E2, defined by Eq. (47), for $0 \leq y \leq 1$ at $x = 0.5$ corresponding to the same test problem considered in Fig. 2.

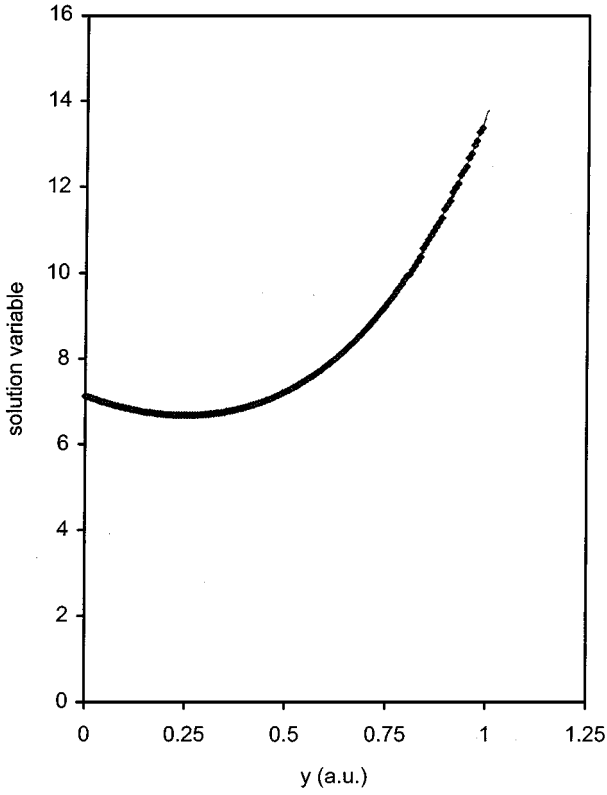

FIG. 4. Comparison of numerical solution (solid line) and analytical solution (symbols), ϕ and Ψ, respectively, for $0 \leq y \leq 1$ at $x = 0.5$ corresponding to the test problem considered in Fig. 2.

evaluate the error indicator $E1$, the relative error $E2$, and the behaviour of the solution variable ϕ in the computational domain.

The first test case has the following values for the coefficients: $A_1 = 1.0$, $A_2 = 1.8$, $A_3 = 1.0$, $A_4 = 2.0$, $A_5 = 2.0$. Figure 2 illustrates the behaviour of the error indicator $E1$ as a function of node density for a symmetric and uniform distribution of nodes in x- and y-directions. In the case considered, since the analytical solution varies exponentially along the diagonal of the computational domain, one would expect a faster decrease in the indicator $E1$ for a higher node density at locations where the solution gradient is large. The relative error in the solution variable as a function of y (for $x = 0.5$) is shown in Fig. 3. The error is less than 0.045% over the range of values, $7 \leq \phi \leq 15$. The appearance of peaks in $E2$ is merely a computational artifact which can be attributed to the Gauss–Seidel iteration scheme and the associated value employed to terminate the iterations. The resulting values of ϕ and its comparison to the analytical solution are shown in Fig. 4 at $x = 0.5$ ($0 \leq y \leq 1$). As expected, following the negligible relative error (see Fig. 3), the discrepancy is less than 0.05%.

The second test case is similar except for a difference in values of the coefficients A_4 and A_5, which now yield a spatial gradient in solution that is larger by a factor of 1000. Here, as before $A_1 = 1.0$, $A_2 = 1.8$, $A_3 = 1.0$, but $A_4 = 8.0$, $A_5 = 8.0$ (see Fig. 5), resulting in the following range in the solution variable: $0 \leq \phi \leq 6000$. Because of the even more dramatic

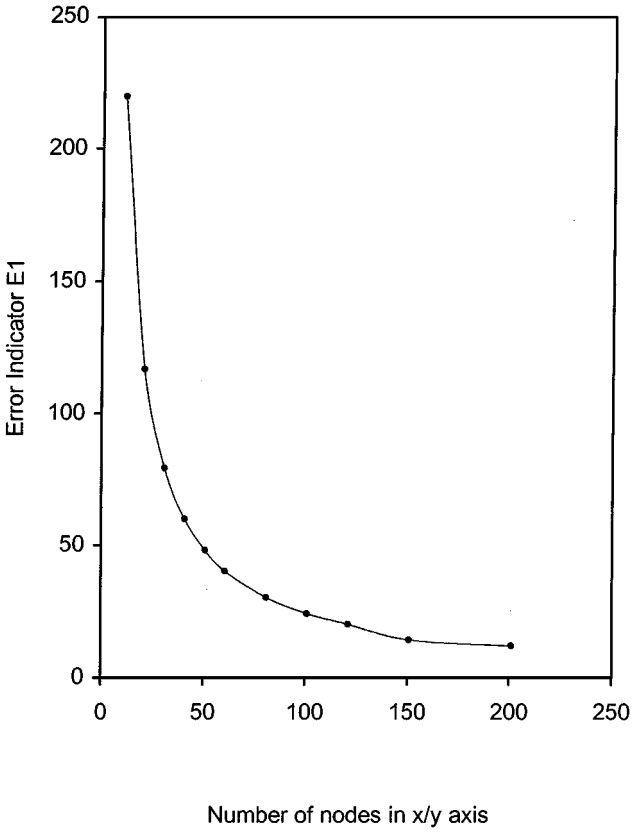

FIG. 5. Same conditions as in Fig. 2, but for the test problem with coefficients $A_1 = 1.0$, $A_2 = 1.8$, $A_3 = 1.0$, $A_4 = 8.0$, $A_5 = 8.0$.

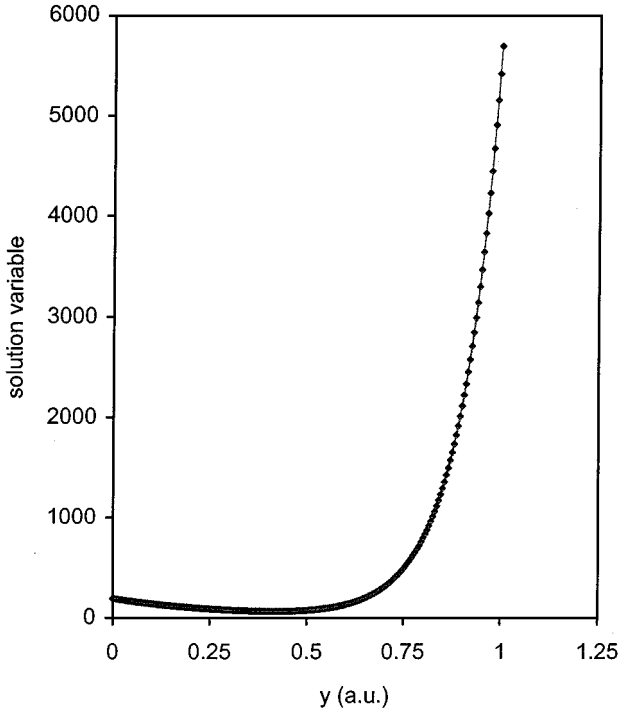

FIG. 6. Same conditions as in Fig. 4, but for the test problem with coefficients $A_1 = 1.0$, $A_2 = 1.8$, $A_3 = 1.0$, $A_4 = 8.0$, $A_5 = 8.0$.

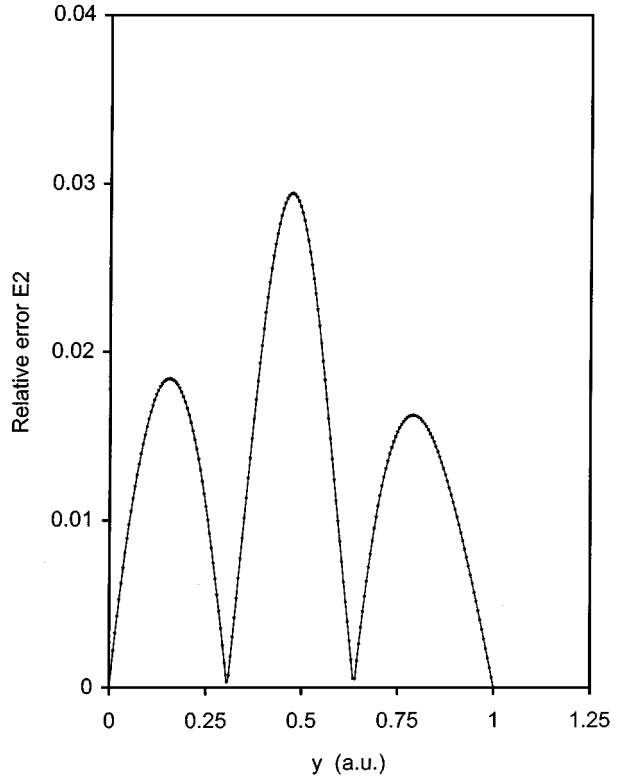

FIG. 7. Same conditions as in Fig. 3, but for the test problem with coefficients $A_1 = 1.0$, $A_2 = 1.8$, $A_3 = 1.0$, $A_4 = 8.0$, $A_5 = 8.0$.

exponential variation of ϕ, the error $E1$, for the same node distribution, is far larger in magnitude. Again we expect that a non-uniform node distribution would result in a faster decrease in $E1$ to account for the large gradient in ϕ. Despite the very large, i.e., more than three orders of magnitude, spread in values of the solution variable (see Fig. 6) coupled with the criterion employed for convergence as given by Eq. (48), the relative error turns to be less than 3% (see Fig. 7). This range of error can be decreased further by a more efficient node distribution and/or through a tighter convergence criterion. Again the observed peaks are numerical artifacts due to the Gauss–Seidel iterative method.

6. CONCLUSIONS

In this paper, we have presented a new discretization scheme for the two-dimensional anisotropic drift-diffusion equation with inhomogeneous coefficients, under steady state conditions. In the diffusion dominated case, a family of schemes is proposed, which preserves the limiting behaviour of the anisotropic elliptic equation and yields an M-matrix. This serves to guarantee a stable oscillation-free solution as well as use of standard iterative solvers. The scheme has been extended to the generalized inhomogeneous drift-diffusion equation whereby we have incorporated the flow of upwind information using a rotated difference method for the drift component. The resulting system of equations satisfies the requirements for an M-matrix. The scheme is validated by comparison with test problems whose exact solutions are known. Good agreement has been observed within physically realistic limits.

REFERENCES

1. A. Nathan and H. Baltes, *Microtransducer CAD* (Springer-Verlag, Vienna, in press).
2. W. Allegretto, A. Nathan, and H. Baltes, Numerical analysis of magnetic field sensitive bipolar devices, *IEEE Trans. Comput. Aided Design* **10**, 501 (1991).
3. T. Manku and A. Nathan, Electrical properties of silicon under nonuniform stress *J. Appl. Phys.* **74**, 1832 (1993).
4. P. I. Crumpton, G. J. Shaw, and A. F. Ware, Discretisation and multigrid solution of elliptic equations with mixed derivative terms and strongly discontinuous coefficients, *J. Comput. Phys.* **116**, 343 (1995).
5. M. F. Wittmaack and W. B. Supan, Positivity preserving in difference schemes for the 2D diffusive transport of atmospheric gases, *J. Comput. Phys.* **115**, 524 (1994).
6. C. S. Tapiero and A. Sulem, Computational aspects in applied stochastic control, *Comput. Econ.* **7**, 109 (1994).
7. P. G. Ciarlet, Discrete maximum principles for finite-difference operators, *Aequationes Math.* **4**, 338 (1970).
8. G. Strang, *Introduction to Applied Mathematics* (Wellesley, MA, 1986).
9. Ch. Hirsh, *Numerical Computation of Internal and External Flows* (Wiley, Chichester, 1988), Vol. 1, p. 191.
10. A. R. Mitchell, *Computational Methods in Partial Differential Equations* (Wiley, London, 1977).
11. F. J. Asencor and M. Panizo, Finite-difference operators in anisotropic inhomogeneous dielectrics: General case, *J. Comput. Phys.* **95**, 387 (1991).
12. J. G. Rice and R. J. Schnipke, A monotone streamline upwind finite element method for convection dominated flows, *Comput. Methods Appl. Mech. Eng.* **48**, 313 (1985).
13. P. L. Roe and D. Sidilkover, Optimum positive linear schemes for advection in two and three dimensions, *SIAM J. Numer. Anal.* **29**, 1542 (1992).